ACS OMEGA

Open Access

http://pubs.acs.org/journal/acsodf

Article

Antiradical Activity of Lignans from *Cleistanthus sumatranus*: Theoretical Insights into the Mechanism, Kinetics, and Solvent Effects

Mai Van Bay, Pham Cam Nam, Nguyen Thi Hoa, Adam Mechler, and Quan V. Vo*

Cite This: *ACS Omega* 2023, 8, 38668−38675

Read Online

ACCESS | Metrics & More | Article Recommendations | Supporting Information

ABSTRACT: Sumatranus lignans (**SL**) isolated from *Cleistanthus sumatranus* have demonstrated bioactivities, e.g., they were shown to exhibit immunosuppressive properties in previous research. Their structure suggests potential antioxidant activity that has not attracted any attention thus far. Consistently, a comprehensive analysis of the antioxidant activity of these compounds is highly desirable with the view of prospective medical applications. In this work, the mechanism and kinetics of the antiradical properties of **SL** against hydroperoxyl radicals were studied by using calculations based on density functional theory (DFT). In the lipid medium, it was discovered that **SL** reacted with HOO$^{\bullet}$ through the formal hydrogen transfer mechanism with a rate constant of $10^{1}-10^{5}$ M^{-1} s^{-1}, whereas in aqueous media, the activity primarily occurred through the sequential proton loss electron transfer mechanism with rate constants of $10^{2}-10^{8}$ M^{-1} s^{-1}. In both lipidic and aqueous environments, the antiradical activity of compounds **6** and **7** exceeds that of resveratrol, ascorbic acid, and Trolox. These substances are therefore predicted to be good radical scavengers in physiological environments.

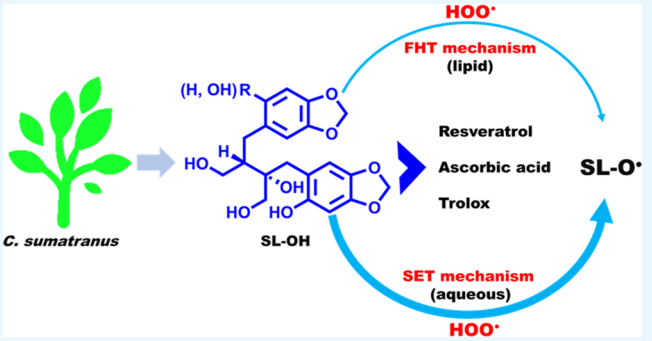

1. INTRODUCTION

Cleistanthus sumatranus is an evergreen tree species that thrives in South China and Southeast Asia.[1] The Cleistanthus genus is rich in beneficial phytochemicals such as phenolic compounds, lignans, alkaloid glucosides, and terpenoids, delivering a vast array of bioactivities such as anticancer and antioxidant properties.[2−7] Consequently, the genus has long attracted the interest of medicinal chemists and pharmacologists.[8,9]

Oxidative stress arises as a result of the disparity between the generation and use of in biological systems.[10] Free radicals, specifically reactive oxygen species (i.e., RO RO$^{\bullet}$(HO$^{\bullet}$), ROO$^{\bullet}$(HOO$^{\bullet}$), $O_2^{\bullet-}$, etc.) and reactive nitrogen species (NO, NO_2, etc.), are implicated as the main drivers of oxidative stress. These entities have a high degree of reactivity and possess the capacity to initiate cascading reactions, hence facilitating the propagation of molecular harm.[10,11] The HO$^{\bullet}$ radical has the highest reactivity and electrophilicity among reactive oxygen species.[12] HO$^{\bullet}$ is implicated as the primary source of oxidative damage to DNA and the majority of tissue damage resulting from exposure to ionizing radiation.[13,14] Nevertheless, this radical exhibits comparable reaction rates to a diverse range of molecules, often approaching or reaching the diffusion limit.[11] The HOO$^{\bullet}$ radical is the most fundamental among the biologically significant ROO$^{\bullet}$ (peroxy) radicals. Efficient elimination of these radicals is a straightforward way of mitigating oxidative stress inside biological systems.[15] The HOO$^{\bullet}$ radical, possessing intermediate reactivity and serving as a prominent target for antioxidant research,[16] has been extensively employed as a standard radical for simulating antioxidant efficacy in both lipid and polar media.[11,17−19]

A recent work reported on the isolation and evaluation of the biological activity of 10 sumatranus lignans (**SL**, **1**−**10**) isolated from *C. sumatranus* (Figure 1).[2] According to immunosuppressive tests, compounds **1**−**3**, **6**, **7**, and **9** had inhibitory effects on the growth of T cells stimulated by ConA with IC_{50} values of 10.1−56.2 μM and the growth of B cells stimulated by LPS with IC_{50} values ranging from 2.7 to 32.8 μM. The proliferation of B lymphocytes was moderately inhibited by compounds **3** and **9**, with IC_{50} values of 2.7 and 3.9 μM, respectively. These compounds would have potent antioxidant properties as members of the lignan family;[20−22] however, their radical scavenging properties have not been investigated yet.

The predictive ability of computational techniques has significantly increased along with enormous advancements in

Received: August 12, 2023
Accepted: September 22, 2023
Published: October 4, 2023

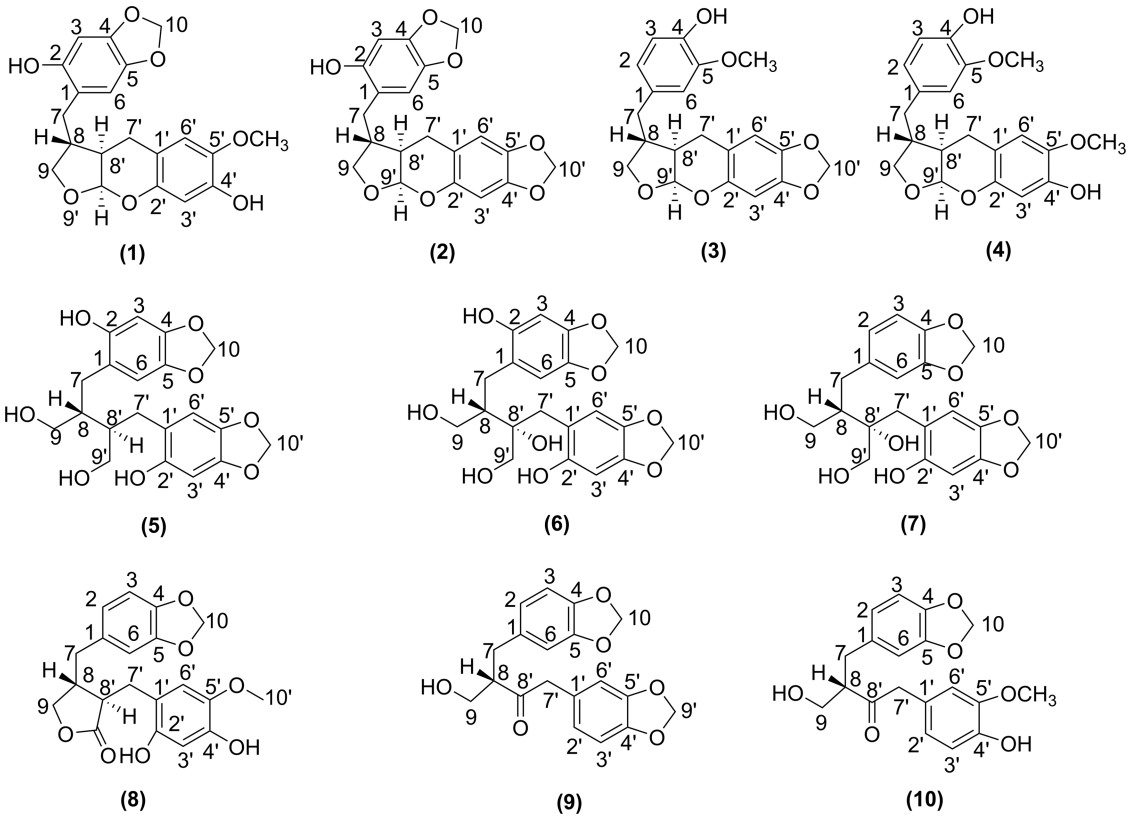

Figure 1. Molecular structure and atomic numbering of **SL**.

computing power in recent years. In silico analysis became a popular approach for evaluating the potential antioxidant properties of the suspected compounds. Impressive advancements in computing power have also accompanied in silico research. In comparison to experimental methods, computational procedures offer knowledge that is reasonably accurate while also requiring less time and money.[11,17,19,23−26] Due to the paucity of standard samples, the experimental evaluation of the antioxidant activity of novel natural products, i.e., **SL**, is a difficult task. However, computational research could effectively address this issue. Thus, the purpose of this study is to investigate, using kinetic and thermodynamic models, the impact of solvent environments and different molecular structures on the antioxidant properties and resistance to oxidation caused by the HOO$^{\bullet}$ radicals of **SL**.

2. RESULTS AND DISCUSSION

2.1. HOO$^{\bullet}$ Antiradical Activity of SL in the Gas Phase.

2.1.1. Thermodynamic Evaluation. The first step in determining the antioxidant activity was to determine the thermochemical properties (bond dissociation enthalpy (BDE), ionization energy (IE) and proton affinity (PA)) that characterize affinity for the three primary mechanisms of action: formal hydrogen transfer (FHT), sequential electron transfer proton transfer (SETPT), and sequential proton loss electron transfer (SPLET), respectively.[23,27−30] The thermochemical parameters of all potential X−H (X = C, O) bonds in the gas phase have been calculated and are given in Table 1.

The BDE (X−H) values range from 77.4 to 111.9 kcal/mol, as shown in Table 1. The **9**-C7′−H bond has the lowest BDE (C−H) bond energy with a value of 81.8 kcal/mol, while the **5**-O2′−H bond has the lowest O−H bond energy, with a value of 77.4 kcal/mol. In the gas phase, the calculated PA and IE values ranged from 315.1 to 346.8 kcal/mol and 117.0 to 230.6 kcal/mol, respectively. Compound **4** possesses the lowest IE value, while the O2′−H bond in compound **7** possesses the lowest PA value. However, the BDEs are significantly lower than those of IE and PA; therefore, the FHT reaction is the primary radical scavenging pathway of **SL** in the gas phase.

To determine which antioxidant pathway the substances follow, the free energy (ΔG°) of HOO$^{\bullet}$ quenching of the phenolic compounds after each mechanism was measured and is recorded in Table 1. Only the FHT mechanism generates negative ΔG° values (or $\Delta G^{\circ} \approx 0$), while neither the SETPT nor SPLET mechanisms are spontaneous (ΔG° = 133.5−197.5 kcal/mol). Hence, the FHT pathway is recognized as the predominant mechanism for neutral SL radical capture in a vacuum environment. Thus, the kinetics should be investigated following this mechanism.

2.1.2. Kinetic Study. In this section, the hydrogen transfer of the O−H and C−H bonds was the primary focus of the kinetic investigation. Figures 2, 3, and Table 2, and depict the potential energy surfaces (PES), kinetic parameters, and optimized TS structures in the gas phase, respectively.

According to PES analysis, the kinetic analysis of reactions typically begins with the consideration of reaction complexes (RCs) that exhibit greater stability than the reactants. These complexes have H-abstraction energies ranging from −12.0 to −3.7 kcal/mol for X−H (X = O, C) bonds. In the FHT mechanism, the reactions can proceed from the RCs to the transition states (TS). Energy barriers for TSs are between 8.7 and 19.7 kcal/mol, which are higher than those for RCs. Before forming products (P), these reactions produce postcomplexes (PCs). The HOO$^{\bullet}$ antiradical of the **5**-O2′−H bond possesses

https://doi.org/10.1021/acsomega.3c05964
ACS Omega 2023, 8, 38668−38675

Table 1. BDE, PA, and IE Values (in kcal/mol) and the ΔG^{o} (in kcal/mol) of the SL + HOO$^{\bullet}$ Reactions via the Single Electron Transfer (SET), Proton Loss (PL), and FHT Processes

	FHT XH + HOO$^{\bullet}$ → X$^{\bullet}$ + HOOH			PL XH + HOO$^{\bullet}$ → X^{-} + HOOH$^{\bullet+}$			SET XH + HOO$^{\bullet}$ → XH$^{\bullet+}$ + HOO^{-}	
comp.	positions	BDE	ΔG^{o}	positions	PA	ΔG^{o}	IE	ΔG^{o}
1	O2−H	83.7	−3.3	O2−H	338.5	188.3	176.2	144.4
	O4′−H	88.9	2.3	O4′−H	342.5	193.7		
	C7−H	92.2	5.3	C7−H				
	C7′−H	85.6	−1.9	C7′−H				
2	O2−H	83.5	−3.2	O2−H	337.8	187.9	177.1	145.2
	C7−H	95.6	9.3	C7−H				
	C7′−H	86.9	0.7	C7′−H				
3	O4−H	86.9	1.6	O4−H	344.8	195.7	230.6	145.9
	C7−H	88.2	2.8	C7−H				
	C7′−H	83.1	−3.1	C7′−H				
4	O4−H	111.9	26.7	O4−H	345.1	195.8	117.0	145.8
	O4′−H	86.1	0.77	O4′−H	345.4	196.2		
	C7−H	88.2	2.8	C7−H				
	C7′−H	82.8	−3.2	C7′−H				
5	O2−H	88.7	1.9	O2−H	341.6	192.0	172.3	135.2
	O2′−H	77.4	−8.1	O2′−H				
	C7−H	96.0	9.9	C7−H				
	C7′−H	97.9	11.5	C7′−H				
6	O2−H	88.2	1.3	O2−H	330.1	181.5	175.1	133.5
	O2′−H	78.5	−7.1	O2′−H	315.1	167.6		
	C7−H	97.1	10.6	C7−H				
	C7′−H	91.8	6.1	C7′−H				
7	O2′−H	78.3	−7.4	O2′−H	317.7	170.2	185.3	146.1
	C7−H	89.0	3.4	C7−H				
	C7′−H	95.2	8.6	C7′−H				
8	O2′−H	87.1	0.2	O2′−H	330.1	181.5	221.1	142.4
	O4′−H	86.9	1.6	O4′−H	346.8	197.5		
	C7−H	87.7	2.1	C7−H				
	C7′−H	87.9	2.6	C7′−H				
9	C7−H	89.5	4.1	C7−H			188.2	153.1
	C7′−H	81.8	−1.0	C7′−H				
10	O4′−H	87.4	2.2	O4′−H	341.4	192.5	200.1	157.1
	C7−H	87.7	2.6	C7−H				
	C7′−H	82.3	−0.4	C7′−H				

the lowest measured TS energy (0.6 kcal/mol), which corresponds to the lowest predicted BDE value for O−H bonds (77.4 kcal/mol).

As per Table 2, the rate constants in the gas phase for **SL** + HOO$^{\bullet}$ reactions range from 8.19×10^{1} to 2.10×10^{7} $M^{-1}s^{-1}$, and their $\Delta G^{\ddagger}$ values are between 11.4 and 21.2 kcal/mol. The tunneling corrections (κ) range between 24.1 and 523.3 for the HOO$^{\bullet}$ radical scavenging. These values, therefore, have a significant effect on the rate constants. Compounds **5**, **6**, **7**, and **8** exhibited good HOO$^{\bullet}$ radical scavenging activity with a rate constant of k_{Eck} = 10^{6}−10^{7} M^{-1} s^{-1}, while compound **9** exhibited the lowest HOO$^{\bullet}$ antiradical trapping with k_{Eck} = 8.19×10^{1} M^{-1} s^{-1}. Compounds **1**, **2**, **3**, **4**, and **10** exhibited a moderate level of hydroperoxyl antiradical activity, as evidenced by their rate constants being within the range of 10^{3} to 10^{5} M^{-1} s^{-1}. The antiradical activity of **SL** was determined by the H-abstraction of the O−H bonds in the majority of the studied compounds, with the exception of compounds **3** and **4**. In these compounds, the H-abstraction of the C7′−H bond accounted for between 42.7 and 49.8% of the overall rate constants. It should be noted that the HOO$^{\bullet}$ radical scavenging activity of compounds **5**, **7**, and **8** in the gas phase is comparable to that of Trolox (k_{ECk} = 1.87×10^{5} M^{-1} s^{-1})[19] the reference antioxidant.

2.2. HOO$^{\bullet}$ Antiradical Activity of SL in Physiological Environments. *2.2.1. Acid−Base Equilibrium.* In polar environments such as water, the radical trapping activity of neutral acidic forms is frequently overshadowed by their ionic states.[30,31] In order to determine the most probable radical scavenging mechanisms, the protonation of **SL** water at pH 7.40 was initially investigated. Due to the fact that the structure of **SL** permits protonation at the O−H bonds with the lowest Gibbs free energy values (Table S2, SI), the pK_a values of **SL** were derived from the literature[32] and are shown in Table 3. The calculated values for pK_a range from 8.22 to 10.92. The range of values for f(HA) is between 0.869 and 1.000, while the range for $f(A^{-})$ is between 0.000 and 0.131. Therefore, in 7.4 pH water, **SLs** exist in both the ionic and neutral states. Thus, in water at physiological pH, these two states were examined in further investigation, whereas in nonpolar media such as pentyl ethanoate solvent, the neutral state should be used to compute the kinetics.

2.2.2. Kinetic Study. The kinetics of **SL** + HOO$^{\bullet}$ reactions in aqueous media were determined for all states by employing

https://doi.org/10.1021/acsomega.3c05964
ACS Omega 2023, 8, 38668−38675

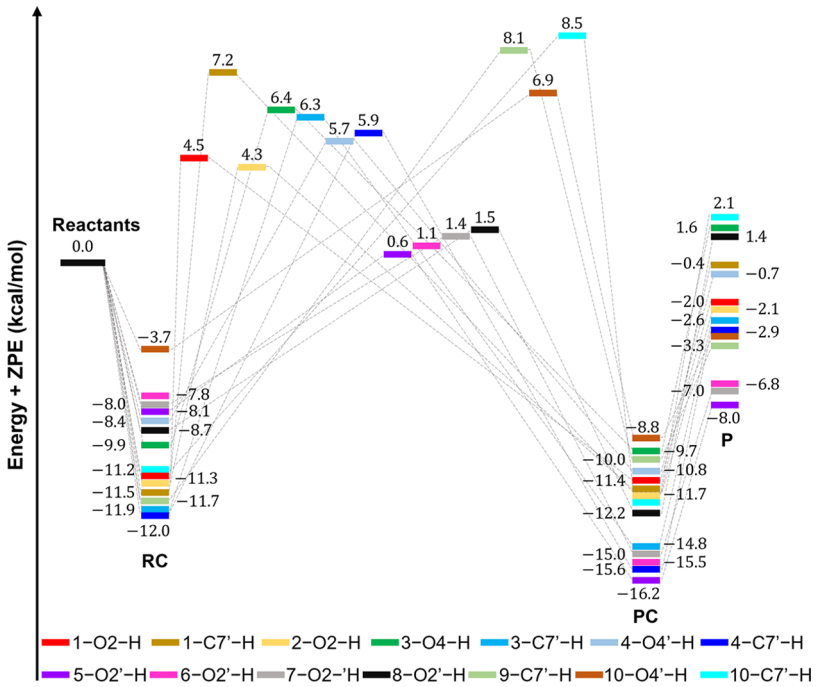

Figure 2. Potential energy surfaces of the **SL** + HOO• reactions.

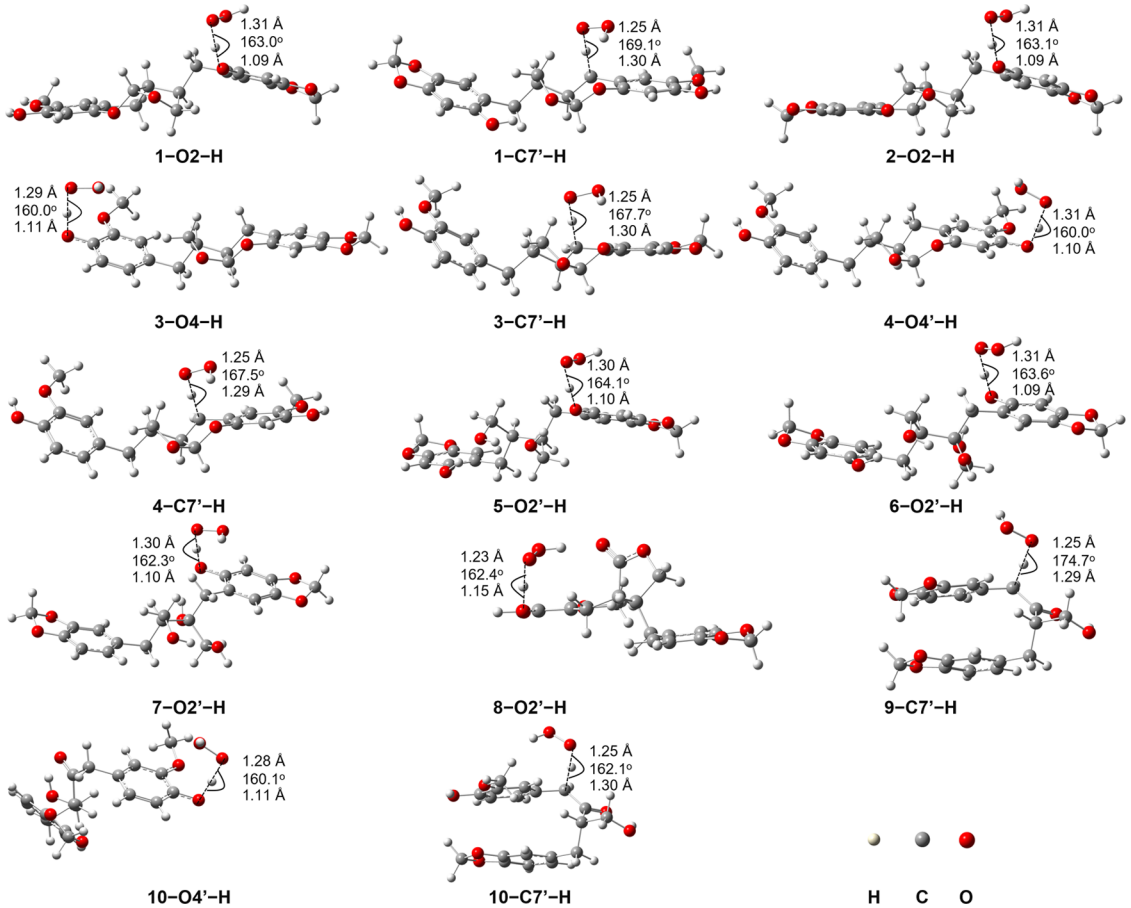

Figure 3. Hydrogen transfer transition states.

the chosen FHT reaction mechanism for neutral states and the SET reaction mechanism for anion states, consistent with prior investigations on phenolic compounds.[18] The thermodynamic analysis in the studied solvents (Table S3, SI) also confirmed that the HOO• radical scavenging activity of the neutral states only occurred following the FHT reactions at similar positions

https://doi.org/10.1021/acsomega.3c05964
ACS Omega 2023, 8, 38668−38675

Table 2. Calculated $\Delta G^{\neq}$ (kcal/mol), Tunneling Corrections (κ), k_{Eck}, and $k_{overall}$ (M^{-1} s^{-1}) for the Reactions between SL and HOO• Radicals

comp.	positions	$\Delta G^{\ddagger}$	κ	k_{Eck}	$k_{overall}$	Γ
1	O2−H	14.3	71.5	3.47×10^5	3.49×10^5	99.5
	C7′−H	18.1	241.3	1.90×10^3		0.5
2	O2−H	14.1	64.6	4.38×10^5	4.38×10^5	100.0
3	O4−H	16.9	180.1	1.04×10^4	1.82×10^4	57.3
	C7′−H	17.5	326.1	7.75×10^3		42.7
4	O4′−H	16.6	123.7	1.23×10^4	2.45×10^4	50.2
	C7′−H	17.2	308.5	1.22×10^4		49.8
5	O2′−H	11.4	28.9	2.10×10^7	2.10×10^7	100.0
6	O2′−H	11.9	24.1	6.91×10^6	6.91×10^6	100.0
7	O2′−H	12.0	41.0	1.07×10^7	1.07×10^7	100.0
8	O2′−H	12.9	273.5	1.55×10^7	1.55×10^7	100.0
9	C7′−H	20.1	301.2	8.19×10^1	8.19×10^1	100.0
10	O4′−H	18.0	155.0	1.48×10^3	1.50×10^3	98.5
	C7′−H	21.2	523.3	2.28×10^1		1.5

$k_{overall} = \Sigma k_{Eck}$

Table 3. Acid Dissociation Equilibrium and Molar Fractions (f) Values of SL at pH = 7.4

comp.	positions	pK_a	f(HA)	f(A^-)
1	O2−H	9.62	0.994	0.006
2	O2−H	9.55	0.993	0.007
3	O4−H	9.87	0.997	0.003
4	O4′−H	9.84	0.996	0.004
5	O2−H	10.92	1.000	0.000
6	O2′−H	8.41	0.911	0.089
7	O2′−H	8.22	0.869	0.131
8	O4′−H	9.81	0.996	0.004
10	O4′−H	9.87	0.997	0.003

in the gas phase. Thus, in the studied media, the overall rate constants ($k_{overall}$) were determined according to eqs 1 and 2, and the overall rate constants ($k_{overall}$) were determined, while the rate constant containing the molar fraction (k_f) was derived using eq 3. Table 4 displays the outcomes.

In pentyl ethanoate solvent

$$k_{overall} = \Sigma k_{app}(\text{FHT} - \text{neutral}) \quad (1)$$

In the aqueous solution

$$k_{overall} = k_f(\text{SET} - \text{anion}) + \Sigma k_f(\text{FHT} - \text{neutral}) \quad (2)$$

$$k_f = k_{app} \cdot f \quad (3)$$

The compounds **1**, **2**, **5**, **6**, **7**, and **8** revealed significant hydroperoxyl radical scavenging action in lipid media, with $k_{overall}$ = 10^4−10^5 M^{-1} s^{-1}, as shown in Table 4. These compounds' antioxidant activity is comparable to that of well-known natural substances including Trolox ($k = 3.40 \times 10^3$ M^{-1} s^{-1}),[33] resveratrol ($k = 1.31 \times 10^4$ M^{-1} s^{-1}),[34] and ascorbic acid ($k = 5.71 \times 10^3$ M^{-1} s^{-1}).[17] However, in the lipid medium, compounds **3**, **4**, **9**, and **10** had only weak hydroperoxyl scavenging properties. According to the calculated results, the HOO• radical trapping ability of **SLs** in the lipid environment can be ranked as follows: **8** ≈ **1** ≈ **2** ≈ **5** ≈ **6** ≈ **7** > **3** > **4** > **9** ≈ **10**.

The SPLET mechanism defined the HOO• radical scavenging activity of **SL** in the aqueous solution with the $\Delta G^{\ddagger}$ = 2.0−4.5 kcal/mol and k_{app}(SET) ≈ k_D, except for compounds **5** and **9**, for which the anion states have not been presented at pH 7.40. Consequently, the HOO• radical trapping ability of compounds **5** and **9** in aqueous solution was determined by the FHT reaction with the lowest $k_{overall}$ values of 6.38×10^4 and 1.60×10^2 M^{-1} s^{-1}, respectively, whereas the other compounds displayed exceptional HOO• trapping activity with $k_{overall}$ = 10^6−10^8 M^{-1} s^{-1}. Compounds **6** and **7** had the greatest activity, with $k_{overall}$ values of 2.23×10^8 and 3.02×10^8 M^{-1} s^{-1}, respectively. This is about 10 times higher than those of **1**, **2**, **3**, **4**, **8**, and **10**. The radical trapping activity of **SL** against HOO• in aqueous solution is ranked as follows: **6** ≈ **7** > **1**, **2**, **3**, **4**, **8**, and **10** > **5** > **9**. In water at the physiological pH, the HOO• trapping activity of **SLs** is about 1 × 10^3 faster than that in the nonpolar solvent. In water at physiological pH, compounds **6** and **7** have a higher HOO• radical scavenging activity than resveratrol ($k = 5.62 \times 10^7$ M^{-1} s^{-1}),[34] ascorbic acid ($k = 9.97 \times 10^7$ M^{-1} s^{-1}),[17] and Trolox ($k = 8.96 \times 10^4$ M^{-1} s^{-1}),[33] whereas compounds **1**, **2**, **3**, **4**, **8**, and **10** are comparable to the references. Thus, the lignans **6**, **7**, and **8** are promising natural antioxidants in the physiological environment.

3. CONCLUSIONS

Using kinetic and thermodynamic models, 10 lignans extracted from *C. sumatranus* were analyzed for their ability to scavenge hydroperoxyl radicals in physiological environments. In nonpolar media, the majority of **SL** activity is mediated by the FHT reaction, whereas the SET mechanism is preferred in polar media. While the activity rate constants in the aqueous solution were around 10^2−10^8 M^{-1} s^{-1}, in the lipid medium, **SL** could react with HOO• *via* the FHT mechanism with a rate constant of 10^1−10^5 M^{-1} s^{-1}. According to the calculated data, the antiradical activity of compounds **6** and **7** is greater than those of resveratrol, ascorbic acid, and Trolox in both lipidic and aqueous environments. In the physiological environment, these substances may therefore function as potent radical scavengers.

4. COMPUTATIONAL DETAILS

The thermochemical features of the compounds (BDE, PA, and IE) were investigated at the M06−2X/6−311++G(d,p) level of theory. Additionally, kinetic parameters, such as activation energies ($\Delta G^{\ddagger}$) in kcal/mol, tunneling corrections (κ), and rate constants (k), were found. The compounds were

https://doi.org/10.1021/acsomega.3c05964
ACS Omega 2023, 8, 38668−38675

Table 4. Calculated $\Delta G^{\neq}$ (kcal/mol), Tunneling Corrections (κ), Rate Constants (k_{app}, k_f, $k_{overall}$, M^{-1} s^{-1}), and Branching Ratios (Γ, %) at 298.15 K for the SL + HOO$^{\bullet}$ Reaction in Water and Pentyl Ethanoate Solvents

			pentyl ethanoate			water					
comp.	mechanisms		$\Delta G^{\ddagger}$	κ	k_{app}	$\Delta G^{\ddagger}$	κ	k_{app}	f	k_f	Γ
1	SET	O2				2.3	18.8[a]	7.80×10^{9}	0.006	4.68×10^{7}	86.8
	FHT	O2	14.4	77.9	1.30×10^{4}	12.5	1661.2	7.18×10^{6}	0.996	7.15×10^{6}	13.2
	$k_{overall}$				**1.30×10^{4}**					**5.39×10^{7}**	
2	SET	O2				2.3	18.5[a]	7.80×10^{9}	0.007	5.46×10^{7}	89.9
	FHT	O2	14.4	72.2	1.16×10^{4}	12.7	2109.5	6.18×10^{6}	0.993	6.14×10^{6}	10.1
	$k_{overall}$				**1.16×10^{4}**					**6.07×10^{7}**	
3	SET	O4				3.1	15.4[a]	6.60×10^{9}	0.003	1.98×10^{7}	99.9
	FHT	O4	16.3	212.6	1.42×10^{3}	15.7	1344.6	2.71×10^{4}	0.997	2.70×10^{4}	0.1
	FHT	C7′	18.8	207.6	2.04×10^{1}	18.3	97.4	2.17×10^{1}	0.997	2.16×10^{1}	0.0
	$k_{overall}$				**1.44×10^{3}**					**1.98×10^{7}**	
4	SET	O4′				2.0	16.9[a]	7.70×10^{9}	0.004	3.08×10^{7}	99.2
	FHT	O4′	16.2	124.2	9.65×10^{2}	14.5	1898.3	2.59×10^{5}	0.996	2.58×10^{5}	0.8
	FHT	C7′	18.8	217.0	2.24×10^{1}	17.5	75.9	7.03×10^{1}	0.996	7.00×10^{1}	0.0
	$k_{overall}$				**9.87×10^{2}**					**3.11×10^{7}**	
5	SET	O2				2.1	18.3[a]	8.00×10^{9}	0.000	0.0	0.0
	FHT	O2′	12.9	29.6	6.24×10^{4}	14.2	281.0	6.38×10^{4}	1.000	6.38×10^{4}	100.0
	$k_{overall}$				**6.24×10^{4}**					**6.38×10^{4}**	
6	SET	O2′				4.4	21.1[a]	2.50×10^{9}	0.089	2.23×10^{8}	99.9
	FHT	O2′	13.0	29.1	5.18×10^{4}	13.4	281.2	2.70×10^{5}	0.911	2.46×10^{5}	0.1
	$k_{overall}$				**5.18×10^{4}**					**2.23×10^{8}**	
7	SET	O2′				4.5	20.4[a]	2.30×10^{9}	0.131	3.01×10^{8}	99.9
	FHT	O2′	13.6	35.1	2.44×10^{4}	13.7	623.8	3.56×10^{5}	0.869	3.09×10^{5}	0.1
	$k_{overall}$				**2.44×10^{4}**					**3.02×10^{8}**	
8	SET	O2′				3.4	16.2[a]	5.90×10^{9}	0.004	2.36×10^{7}	96.4
	FHT	O2′	13.5	165.4	1.32×10^{5}	13.6	1253.0	8.88×10^{5}	0.996	8.84×10^{5}	3.6
	$k_{overall}$				**1.32×10^{5}**					**2.45×10^{7}**	
9	SET										
	FHT	C7′	21.5	323.2	3.48×10^{-1}	18.6	1170.0	1.60×10^{2}	1.000	1.60×10^{2}	100.0
	$k_{overall}$				**3.48×10^{-1}**					**1.60×10^{2}**	
10	SET	O4′				3.9	16.1[a]	4.30×10^{9}	0.003	1.29×10^{7}	100.0
	FHT	O4′	18.0	177.6	7.36×10^{1}	16.7	863.5	2.89×10^{3}	0.997	2.88×10^{3}	0.0
	$k_{overall}$				**7.36×10^{1}**					**1.29×10^{7}**	

[a] λ (kcal/mol); $k_f = f.k_{app}$; $\Gamma = k_f.100/k_{overall}$.

detected in the gaseous phase within the physiological environment, and the lipid medium was observed to contain pentyl ethanoate. Upon comparing this method to other more intricate procedures, such as G3(MP2)-RAD, as well as experimental data, it has been ascertained that this method exhibits a considerable level of accuracy in the calculation of kinetic and thermodynamic parameters, but with modest levels of error.[11,24,31,35,36]

The BDE, PA, and IE values were computed as follows[19,37]

$$\mathrm{BDE} = H(\mathrm{SL}^{\bullet}) + H(H^{\bullet}) - H(\mathbf{SL}-H) \quad (4)$$

$$\mathrm{PA} = H(\mathrm{SL}^{-}) + H(H^{+}) - H(\mathbf{SL}-H) \quad (5)$$

$$\mathrm{IE} = H(\mathbf{SL}-H^{+\bullet}) + H(\mathrm{e}^{-}) - H(\mathbf{SL}-H) \quad (6)$$

The enthalpies of the hydrogen atom, proton, neutral molecule, anion, radical, and cation radical are denoted as $H(H^{\bullet})$, $H(H^{+})$, $H(\mathbf{SL-H})$, $H(\mathbf{SL}^{-})$, $H(\mathbf{SL}^{\bullet})$, and $H(\mathbf{SL-H}^{+\bullet})$, respectively.

The kinetic calculations were conducted using the methodology for the quantum mechanics-based test for overall free radical scavenging activity (QM-ORSA), as indicated by the low error rates (k_{calc}/k_{exp} ratio = 0.3−2.9).[17,30,38,39] The aforementioned assay has been widely employed to assess the radical scavenging activity of antioxidants.[11,17,24,38,40] The rate constant (k) was determined through the application of the conventional transition state theory (TST) using a 1 M standard state.[41−45] Further information and specific calculations may be found in Table S1 in the Supporting Information (SI).

$$k = \sigma k \frac{k_B T}{h} \mathrm{e} - (\Delta G^{\neq})/RT \quad (7)$$

In the given context, k_B and h represent the Boltzmann and Planck constants, respectively. $\Delta G^{\ddagger}$ denotes the Gibbs free energy of activation for the reaction under investigation, while σ represents the reaction symmetry number, which quantifies the degeneracy of the reaction pathway.[46,47] The tunneling adjustments, which were calculated based on the Eckart barrier,[48] are taken into consideration by the parameter κ.

The examination of species with numerous conformers included the conformer that possessed the lowest electronic energy. The distinguishing characteristic of all transition states was the existence of a solitary imaginary frequency. To guarantee proper linkage between each transition state and the precomplex and postcomplex, intrinsic coordinate calculations (IRCs) were performed. Computations were conducted

https://doi.org/10.1021/acsomega.3c05964
ACS Omega 2023, 8, 38668−38675

utilizing the Gaussian 16 suite of programs[49] and the Eyringpy software, depending on the specific case.[50,51]

■ ASSOCIATED CONTENT

Supporting Information

The Supporting Information is available free of charge at https://pubs.acs.org/doi/10.1021/acsomega.3c05964.

Thermodynamic parameters; Cartesian coordinates, frequency, and energies of all of the transition states (PDF)

■ AUTHOR INFORMATION

Corresponding Author

Quan V. Vo − *The University of Danang - University of Technology and Education, Danang 550000, Vietnam;* orcid.org/0000-0001-7189-9584; Email: vvquan@ute.udn.vn, vovanquan1980@gmail.com

Authors

Mai Van Bay − *The University of Danang - University of Science and Education, Danang 550000, Vietnam*

Pham Cam Nam − *The University of Danang - University of Science and Technology, Danang 550000, Vietnam;* orcid.org/0000-0002-7257-544X

Nguyen Thi Hoa − *The University of Danang - University of Technology and Education, Danang 550000, Vietnam*

Adam Mechler − *Department of Biochemistry and Chemistry, La Trobe University, Victoria 3086, Australia;* orcid.org/0000-0002-6428-6760

Complete contact information is available at: https://pubs.acs.org/10.1021/acsomega.3c05964

Notes

The authors declare no competing financial interest.

■ ACKNOWLEDGMENTS

This research is funded by Funds for Science and Technology Development of the University of Danang under project number B2020-DN03-47 (M.V.B).

■ REFERENCES

(1) Lountos, G. T.; Jiang, R.; Wellborn, W. B.; Thaler, T. L.; Bommarius, A. S.; Orville, A. M. The crystal structure of NAD(P)H oxidase from Lactobacillus sanfranciscensis: insights into the conversion of O2 into two water molecules by the flavoenzyme. *Biochemistry* **2006**, *45* (32), 9648−9659.

(2) Zhou, J.-S.; Yao, J.-Y.; Gao, Y.; Liu, Q.-F.; Zhou, B.; He, S.-J.; Zhao, J.-X.; Yue, J.-M. Sumatranins A−J: Lignans with Immunosuppressive Activity from *Cleistanthus sumatranus*. *J. Nat. Prod.* **2023**, *86*, 1606−1614, DOI: 10.1021/acs.jnatprod.3c00300.

(3) Nguyen, L. H.; Vu, V. N.; Phi Thi, D.; Tran, V. H.; Litaudon, M.; Roussi, F.; Nguyen, V. H.; Chau, V. M.; Doan Thi Mai, H.; Pham, V. C. Cytotoxic lignans from fruits of Cleistanthus tonkinensis. *Fitoterapia* **2020**, *140*, No. 104432.

(4) Pinho, P. M. M.; Kijjoa, A. Chemical constituents of the plants of the genus Cleistanthus and their biological activity. *Phytochem. Rev.* **2007**, *6*, 175−182.

(5) Thanh, V. T. T.; Pham, V. C.; Nguyen, H. H.; Mai, H. D. T.; Minh, H. N. T.; Nguyen, V. H.; Litaudon, M.; Gueritte, F.; Chau, V. M. *Cleistanone: A Triterpenoid from Cleistanthus indochinensis with a New Carbon Skeleton*; Wiley Online Library, 2011.

(6) Trinh Thi Thanh, V.; Cuong Pham, V.; Doan Thi Mai, H.; Litaudon, M.; Gueritte, F.; Retailleau, P.; Nguyen, V. H.; Chau, V. M. Cytotoxic lignans from fruits of *Cleistanthus indochinensis*: synthesis of cleistantoxin derivatives. *J. Nat. Prod.* **2012**, *75* (9), 1578−1583.

(7) Fan, S.-r.; Guo, J.-j.; Wang, Y.-t.; Yang, B.-j.; Chen, D.-z.; Hao, X.-j. Two new bioactive lignans from leaves and twigs of Cleistanthus concinnus Croizat. *Nat. Prod. Res.* **2020**, *34* (23), 3328−3334.

(8) Jearawuttanakul, K.; Khumkhrong, P.; Suksen, K.; Reabroi, S.; Munyoo, B.; Tuchinda, P.; Borwornpinyo, S.; Boonmuen, N.; Chairoungdua, A. Cleistanthin A induces apoptosis and suppresses motility of colorectal cancer cells. *Eur. J. Pharmacol.* **2020**, *889*, No. 173604.

(9) Pradheepkumar, C. P.; Panneerselvam, N.; Shanmugam, G. Cleistanthin A causes DNA strand breaks and induces apoptosis in cultured cells. *Mutat. Res., Genet. Toxicol. Environ. Mutagen.* **2000**, *464* (2), 185−193.

(10) Sayre, L. M.; Perry, G.; Smith, M. A. Oxidative stress and neurotoxicity. *Chem. Res. Toxicol.* **2008**, *21* (1), 172−188.

(11) Galano, A.; Raúl Alvarez-Idaboy, J. Computational strategies for predicting free radical scavengers' protection against oxidative stress: Where are we and what might follow? *Int. J. Quantum Chem.* **2019**, *119* (2), No. e25665.

(12) Pryor, W. A. Why is the hydroxyl radical the only radical that commonly adds to DNA? Hypothesis: it has a rare combination of high electrophilicity, high thermochemical reactivity, and a mode of production that can occur near DNA. *Free Radic. Biol. Med.* **1988**, *4* (4), 219−223.

(13) Galano, A.; Alvarez-Idaboy, J. R. Guanosine+ oh radical reaction in aqueous solution: A reinterpretation of the uv− vis data based on thermodynamic and kinetic calculations. *Org. Lett.* **2009**, *11* (22), 5114−5117.

(14) Vijayalaxmi; Reiter, R. J.; Tan, D.-X.; Herman, T. S.; Thomas, C. R., Jr. Melatonin as a radioprotective agent: a review. *Int. J. Radiat. Oncol., Biol. Phys.* **2004**, *59* (3), 639−653.

(15) Terpinc, P.; Abramovič, H. A kinetic approach for evaluation of the antioxidant activity of selected phenolic acids. *Food Chem.* **2010**, *121* (2), 366−371.

(16) Masuda, T.; Yamada, K.; Maekawa, T.; Takeda, Y.; Yamaguchi, H. Antioxidant mechanism studies on ferulic acid: identification of oxidative coupling products from methyl ferulate and linoleate. *J. Agric. Food Chem.* **2006**, *54* (16), 6069−6074.

(17) Galano, A.; Alvarez-Idaboy, J. R. A Computational Methodology for Accurate Predictions of Rate Constants in Solution: Application to the Assessment of Primary Antioxidant Activity. *J. Comput. Chem.* **2013**, *34* (28), 2430−2445.

(18) Vo, Q. V.; Hoa, N. T.; Thong, N. M.; Mechler, A. The hydroperoxyl and superoxide anion radical scavenging activity of anthocyanidins in physiological environments: Theoretical insights into mechanisms and kinetics. *Phytochemistry* **2021**, *192*, No. 112968.

(19) Boulebd, H.; Amine Khodja, I.; Bay, M. V.; Hoa, N. T.; Mechler, A.; Vo, Q. V. Thermodynamic and Kinetic Studies of the Radical Scavenging Behavior of Hydralazine and Dihydralazine: Theoretical Insights. *J. Phys. Chem. B* **2020**, *124*, 4123−4131, DOI: 10.1021/acs.jpcb.0c02439.

(20) Touré, A.; Xueming, X. Flaxseed lignans: source, biosynthesis, metabolism, antioxidant activity, bio-active components, and health benefits. *Compr. Rev. Food Sci. Food Saf.* **2010**, *9* (3), 261−269.

(21) Saleem, M.; Kim, H. J.; Ali, M. S.; Lee, Y. S. An update on bioactive plant lignans. *Nat. Prod. Rep.* **2005**, *22* (6), 696−716.

(22) Wan, Y.; Li, H.; Fu, G.; Chen, X.; Chen, F.; Xie, M. The relationship of antioxidant components and antioxidant activity of sesame seed oil. *J. Sci. Food Agric.* **2015**, *95* (13), 2571−2578.

(23) Ingold, K. U.; Pratt, D. A. Advances in radical-trapping antioxidant chemistry in the 21st century: a kinetics and mechanisms perspective. *Chem. Rev.* **2014**, *114* (18), 9022−9046.

(24) Carreon-Gonzalez, M.; Vivier-Bunge, A.; Alvarez-Idaboy, J. R. Thiophenols, Promising Scavengers of Peroxyl Radicals: Mechanisms and kinetics. *J. Comput. Chem.* **2019**, *40*, 2103−2110, DOI: 10.1002/jcc.25862.

(25) Vandenbussche, S.; Díaz, D.; Fernández-Alonso, M. C.; Pan, W.; Vincent, S. P.; Cuevas, G.; Cañada, F. J.; Jiménez-Barbero, J.;

Bartik, K. Aromatic−carbohydrate interactions: an NMR and computational study of model systems. *Chem. − Eur. J.* **2008**, *14* (25), 7570−7578.
(26) Canales, A.; Rodríguez-Salarichs, J.; Trigili, C.; Nieto, L.; Coderch, C.; Andreu, J. M.; Paterson, I.; Jiménez-Barbero, J.; Díaz, J. F. Insights into the interaction of discodermolide and docetaxel with tubulin. Mapping the binding sites of microtubule-stabilizing agents by using an integrated NMR and computational approach. *ACS Chem. Biol.* **2011**, *6* (8), 789−799.
(27) Litwinienko, G.; Ingold, K. Solvent effects on the rates and mechanisms of reaction of phenols with free radicals. *Acc. Chem. Res.* **2007**, *40* (3), 222−230.
(28) Litwinienko, G.; Ingold, K. Abnormal solvent effects on hydrogen atom abstraction. 2. Resolution of the curcumin antioxidant controversy. The role of sequential proton loss electron transfer. *J. Org. Chem.* **2004**, *69* (18), 5888−5896.
(29) Galano, A.; Mazzone, G.; Alvarez-Diduk, R.; Marino, T.; Alvarez-Idaboy, J. R.; Russo, N. Food antioxidants: chemical insights at the molecular level. *Annu. Rev. Food Sci. Technol.* **2016**, *7*, 335−352.
(30) Vo, Q. V.; Bay, M. V.; Nam, P. C.; Quang, D. T.; Flavel, M.; Hoa, N. T.; Mechler, A. Theoretical and Experimental Studies of the Antioxidant and Antinitrosant Activity of Syringic Acid. *J. Org. Chem.* **2020**, *85* (23), 15514−15520.
(31) Galano, A.; Alvarez-Idaboy, J. R. Kinetics of radical-molecule reactions in aqueous solution: A benchmark study of the performance of density functional methods. *J. Comput. Chem.* **2014**, *35* (28), 2019−2026.
(32) Galano, A.; Pérez-González, A.; Castañeda-Arriaga, R.; Muñoz-Rugeles, L.; Mendoza-Sarmiento, G.; Romero-Silva, A.; Ibarra-Escutia, A.; Rebollar-Zepeda, A. M.; León-Carmona, J. R.; Hernández-Olivares, M. A.; Alvarez-Idaboy, J. R. Empirically Fitted Parameters for Calculating p K a Values with Small Deviations from Experiments Using a Simple Computational Strategy. *J. Chem. Inf. Model.* **2016**, *56* (9), 1714−1724.
(33) Alberto, M. E.; Russo, N.; Grand, A.; Galano, A. A physicochemical examination of the free radical scavenging activity of Trolox: mechanism, kinetics and influence of the environment. *Phys. Chem. Chem. Phys.* **2013**, *15* (13), 4642−4650.
(34) Iuga, C.; Alvarez-Idaboy, J. R. l.; Russo, N. Antioxidant activity of trans-resveratrol toward hydroxyl and hydroperoxyl radicals: a quantum chemical and computational kinetics study. *J. Org. Chem.* **2012**, *77* (8), 3868−3877.
(35) Zhao, Y.; Schultz, N. E.; Truhlar, D. G. Design of Density Functionals by Combining the Method of Constraint Satisfaction with Parametrization for Thermochemistry, Thermochemical Kinetics, and Noncovalent Interactions. *J. Chem. Theory Comput.* **2006**, *2* (2), 364−382.
(36) Zhao, Y.; Truhlar, D. G. How Well Can New-Generation Density Functionals Describe the Energetics of Bond-Dissociation Reactions Producing Radicals? *J. Phys. Chem. A* **2008**, *112* (6), 1095−1099.
(37) Vo, Q. V.; Mechler, A. In silico study of the radical scavenging activities of natural indole-3-carbinols. *J. Chem. Inf. Model.* **2020**, *60* (1), 316−321.
(38) Alvarez-Idaboy, J. R. l.; Galano, A. On the Chemical Repair of DNA Radicals by Glutathione: Hydrogen Vs Electron Transfer. *J. Phys. Chem. B* **2012**, *116* (31), 9316−9325.
(39) Vo, Q. V.; Van, L. T. N.; Hoa, N. T.; Mechler, A. Modelling the mechanism and kinetics of the radical scavenging activity of iminostilbene. *Polym. Degrad. Stab.* **2021**, *185*, No. 109483.
(40) Galano, A. Free radicals induced oxidative stress at a molecular level: the current status, challenges and perspectives of computational chemistry based protocols. *J. Mex. Chem. Soc.* **2015**, *59* (4), 231−262.
(41) Evans, M. G.; Polanyi, M. Some Applications of the Transition State Method to the Calculation of Reaction Velocities, Especially in Solution. *Trans. Faraday Soc.* **1935**, *31*, 875−894.
(42) Eyring, H. The Activated Complex in Chemical Reactions. *J. Chem. Phys.* **1935**, *3* (2), 107−115.
(43) Truhlar, D. G.; Hase, W. L.; Hynes, J. T. Current Status of Transition-State Theory. *J. Phys. Chem. A* **1983**, *87* (15), 2664−2682.
(44) Furuncuoğlu, T.; Ugur, I.; Degirmenci, I.; Aviyente, V. Role of Chain Transfer Agents in Free Radical Polymerization Kinetics. *Macromolecules* **2010**, *43* (4), 1823−1835.
(45) Vélez, E.; Quijano, J.; Notario, R.; Pabón, E.; Murillo, J.; Leal, J.; Zapata, E.; Alarcón, G. A Computational Study of Stereospecifity in the Thermal Elimination Reaction of Menthyl Benzoate in the Gas Phase. *J. Phys. Org. Chem.* **2009**, *22* (10), 971−977.
(46) Pollak, E.; Pechukas, P. Symmetry Numbers, Not Statistical Factors, Should Be Used in Absolute Rate Theory and in Broensted Relations. *J. Am. Chem. Soc.* **1978**, *100* (10), 2984−2991.
(47) Fernández-Ramos, A.; Ellingson, B. A.; Meana-Pañeda, R.; Marques, J. M.; Truhlar, D. G. Symmetry Numbers and Chemical Reaction Rates. *Theor. Chem. Acc.* **2007**, *118* (4), 813−826.
(48) Eckart, C. The Penetration of A Potential Barrier by Electrons. *Phy. Rev.* **1930**, *35* (11), 1303.
(49) Frisch, M. J.; Trucks, G. W.; Schlegel, H. B.; Scuseria, G. E.; Robb, M. A.; Cheeseman, J. R.; Scalmani, G.; Barone, V.; Mennucci, B.; Petersson, G. A.; Nakatsuji, H.; Caricato, M.; Li, X.; Hratchian, H. P.; Izmaylov, A. F.; J Bloino, G. Z.; Sonnenberg, J. L.; Hada, M.; Ehara, M.; Toyota, K.; Fukuda, R.; Hasegawa, J.; Ishida, M.; Nakajima, T.; Honda, Y.; Kitao, O.; Nakai, H.; Vreven, T.; Montgomery, J. A.; J E, P., Jr.; Ogliaro, F.; Bearpark, M.; Heyd, J. J.; Brothers, E.; Kudin, K. N.; Staroverov, V. N.; Keith, T.; Kobayashi, R.; Normand, J.; Raghavachari, K.; Rendell, A.; Burant, J. C.; Iyengar, S. S.; Tomasi, J.; Cossi, M.; Rega, N.; Millam, J. M.; Klene, M.; Knox, J. E.; Cross, J. B.; Bakken, V.; Adamo, C.; Jaramillo, J.; Gomperts, R.; Stratmann, R. E.; Yazyev, O.; Austin, A. J.; Cammi, R.; Pomelli, C.; Ochterski, J. W.; Martin, R. L.; Morokuma, K.; Zakrzewski, V. G.; Voth, G. A.; Salvador, P.; Dannenberg, J. J.; Dapprich, S.; Daniels, A. D.; Farkas, O.; Foresman, J. B.; Ortiz, J. V.; Cioslowski, J.; Fox, D. J. *Gaussian 16*; Revision A.03; Gaussian, Inc.: Wallingford CT, 2016.
(50) Dzib, E.; Cabellos, J. L.; Ortíz-Chi, F.; Pan, S.; Galano, A.; Merino, G. Eyringpy: A Program for Computing Rate Constants in the Gas Phase and in Solution. *Int. J. Quantum Chem.* **2019**, *119* (2), No. e25686.
(51) Dzib, E.; Cabellos, J. L.; Ortiz-Chi, F.; Pan, S.; Galano, A.; Merino, G. *Eyringpy 1.0.2*; Cinvestav: Mérida, Yucatán, 2018.

https://doi.org/10.1021/acsomega.3c05964
ACS Omega 2023, 8, 38668−38675